

Auto-Gopher-2 – An autonomous wireline rotary piezo-percussive deep drilling mechanism

Yoseph Bar-Cohen, Mircea Badescu, Hyeong Jae Lee, Stewart Sherrit, Xiaoqi Bao,
Shannon Jackson, Brandon Metz, and Alan Simonini

Jet Propulsion Laboratory, California Institute of Technology, (MS 67-119), 4800 Oak Grove
Drive, Pasadena, CA 91109-8099, Phone 818-393-5700, Fax 818-393-2879, yosi@jpl.nasa.gov
web: <http://ndea.jpl.nasa.gov>

and

Kris Zacny, Bolek Mellerowicz, Daniel Kim, Gale L Paulsen
Honeybee Robotics Spacecraft Mechanisms Corporation, Pasadena, CA

ABSTRACT

Drilling deep into the subsurface of planetary bodies in the Solar System for samples acquisition enables critical capabilities for future NASA exploration missions in its quest to understand the origins of the Solar System and potentially the search for life. Such planetary bodies as Mars and Europa are key targets for potential missions that would require reaching great depths. Performing drilling while using minimal mass/volume systems and with low energy consumption are the main requirements that are imposed on such technologies. A wireline deep drill, called Auto-Gopher-2, is currently being developed as a joint effort between JPL and Honeybee Robotics Ltd. The Auto-Gopher II is a wireline rotary piezo-percussive deep drilling mechanism that combines formation breaking by rotating and piezoelectric actuator hammering and cuttings removal by rotating a fluted bit. The hammering mechanism is based on the Ultrasonic/Sonic Drill/Corer (USDC) mechanism that has been developed as an adaptable tool for many drilling and coring applications. The USDC uses an intermediate ball-shape free-mass to transform high frequency vibrations of a piezoelectric transducer horn tip into sonic hammering of the drill bit. The lessons learned from the previous studies are being implemented into the development of the Auto-Gopher-II, an autonomous deep wireline drill with integrated cuttings and sample management and drive electronics. Subsystems of the wireline drill are being developed in parallel at JPL and Honeybee Robotics, Ltd. Issues related to the bit and its ability to retain the cuttings for caching and removal are currently being addressed. This paper presents the development efforts of the piezoelectric actuator, cuttings removal and retention flutes and drive electronics.

INTRODUCTION

A deep drill, called Auto-Gopher-2, is currently being developed as both an ice drill, with potential application to Europa or Enceladus, and a regolith and soft rock drill, with potential application to Mars. The Auto-Gopher II is a wireline rotary-hammer drill that uses a combination of formation breaking by hammering via a piezoelectric actuated percussive mechanism as well as cuttings removal by rotating a fluted bit. The percussive mechanism is based on the Ultrasonic/Sonic Drill/Corer (USDC) mechanism that has been developed for many drilling and coring applications [Bar-Cohen, 2001; Sherrit, 2000; Bao, 2003]. The USDC uses a free-mass to transform high frequency vibrations that are generated by the horn tip of a piezoelectric transducer into sonic hammering of the drill bit. The first generation of the implementation of the USDC into a deep

drill utilizing a wireline approach has been the development of the Ultrasonic/Sonic Ice Gopher [Badescu, 2006]. In the Auto-Gopher-I, the percussive mechanism was integrated with rotation [Badescu, 2011, Bar-Cohen and Zacny, 2009]. The drill was demonstrated to reach 3 m in a 40MPa compressive strength gypsum formation, [Zacny et al., 2013]. The lessons learned from these developments are being integrated into the Auto-Gopher-II development, which is a fully autonomous deep wireline drill with integrated cuttings and sample management and drive electronics.

The objective of developing the Auto-Gopher is to demonstrate a scalable technology that makes deep drilling possible using current launch vehicles and power sources. The applicability of the drill dictates the requirements in mass, power and operation effectiveness. As a wireline drill, the Auto-Gopher is essentially cylinder that includes a drive mechanisms, actuators, and bit. The drill is suspended at the end of a lightweight tether and the penetration depth is limited only by the packaging capability of the tether. This enables drilling to greater depths without a significant increase in system mass or complexity.

The available power is one of the limitations for drilling in planetary bodies and the proven power sources for landed missions are solar panels and Radioisotope Thermal Generators (RTG). Drilling with Auto-Gopher through ice using 300 W power consumption can result in 10-20 minutes of drilling per hour. In contrast, an ice melt probe would require kilowatts of power and this requires development of small, space-worthy nuclear reactor, which will be very expensive and take a long time to develop. One of the drawbacks of the wireline system is the possibility of borehole collapse and using casings is complex making the application to a mission prohibitively risky. For this reason, the drilled environment should be restricted to stable formations such as ice or ice-cemented grounds, where the probability of finding life would be highest. In turn, plausible targets may include the Northern and the Southern Polar Regions of Mars, or Enceladus, and Europa. This paper reviews the development efforts of the piezoelectric actuator, drive electronics as well as the cuttings removal and retention bit.

PIEZOELECTRIC ACTUATOR

The percussive action in the Auto-Gopher is generated by a piezoelectric actuator. The actuator consists of a piezoelectric stack that was designed to be driven by 360V that will be provided by the drill bus. The voltage level was selected based on reduction of the power loss for a 1000 m long cable. A titanium (Ti-6Al-4V) stepped dog-bone horn amplifies the vibrations displacement of the piezoelectric stack. PZT (Plumbum, Zirconate, Titanate) rings in the stack are held in compression between the horn base and a backing using a pre-stress bolt. An FEA model of the piezoelectric transducer was generated using Ansys™ (**Figure 1**). This model uses the actuator geometric parameters (such as the length of the piezoelectric stack, the backing, and the horn) that were adjusted to obtain a piezoelectric transducer with a resonant frequency of about 5 kHz. The neutral plane was designed to be collocated with the mounting flange inside the horn base and away from the horn – piezoelectric disks interface. The design and the geometric parameters are shown in **Figure 2** and the materials and their characteristics are listed in **Table 1**.

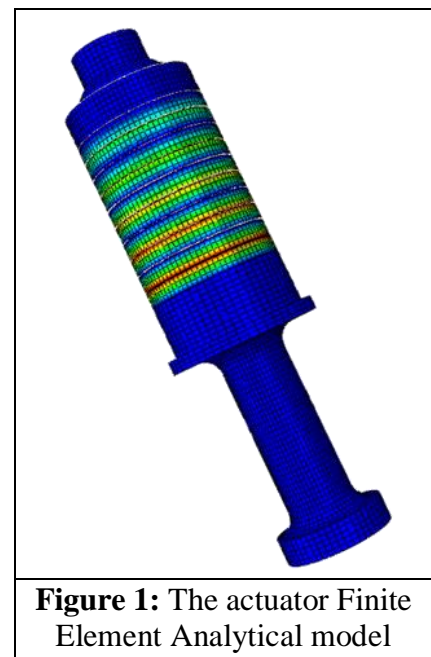


Figure 1: The actuator Finite Element Analytical model

The actuator was assembled and the impedance spectrum was measured and modal analysis of the piezoelectric transducer was performed to identify the mode shapes and natural frequencies of the chosen piezoelectric actuator design. After parts fabrication and actuator assembly the impedance spectra of the actuator were re-measured and the actuator was integrated into a testbed (**Figure 3**). The goal of the testbed was to determine the maximum kinetic energy the striker can acquire after the impact with the transducer horn tip and the frequency of the impact. The testbed includes a vertically mounted plate where the actuator is mounted at the neutral plane flange. The actuator is mounted with the horn tip facing up to eliminate the need of a striker preload spring. A solid rod was used as a bit replacement and was mounted between two high stiffness wave springs preloaded between two plate-mounted collars. The gap between the bit replacement and the striker could be adjusted to determine an optimal value where the striker reaches resonance.

Table 1: Actuator materials

	OD (mm)	ID (mm)	Length (mm)	Young's modulus (GPa)	ρ (kg/m ³)	Poisson's ratio	σ_c (MPa)
Piezo (PZT8)	50.8	21.6	6.35	-	7500	0.3	517 (35)
Backing (Steel)	50.8	18.76	12	205	7850	0.28	250
Horn (Titanium)	30.0	6.00	68	116	4506	0.34	970 (880)

The bit diameter and the size of the teeth contact area suggest that the striker impact energy be larger than 1J. Preliminary testing with the 10 kHz actuator showed striker impact energy smaller than the desired minimum value and a decision was made to redesign the actuator to have larger horn tip displacement and this required a larger piezoelectric stack. The redesigned actuator has included additional alumina disks that insulate electrically the piezoelectric stack electrodes from the transducer horn, backing and stress bolt allowing the ground to float. These insulators were integrated to match the interface dictated by the whole system drill design. A photograph of the assembled actuator is shown in **Figure 4**. The alumina insulation is in addition to the Teflon that is used to wrap on the stress bolt.

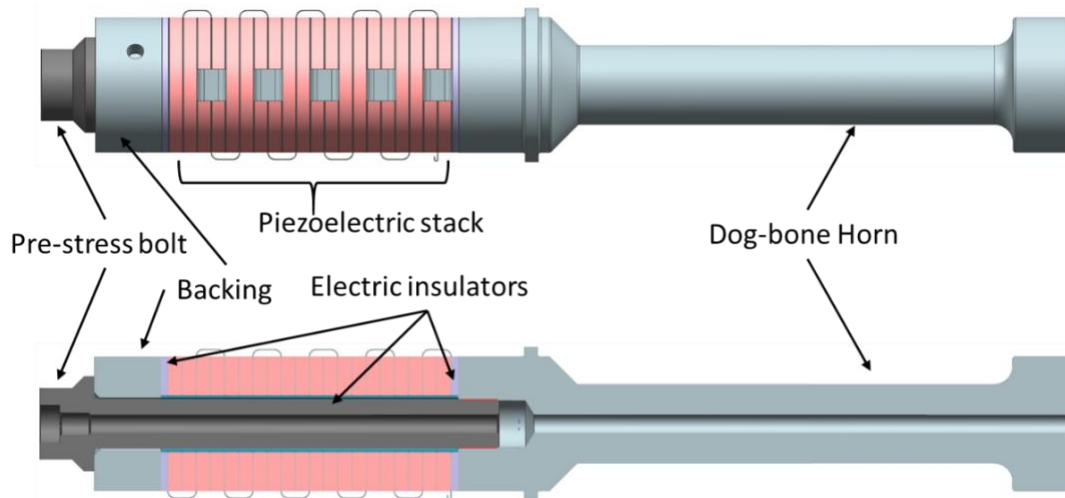
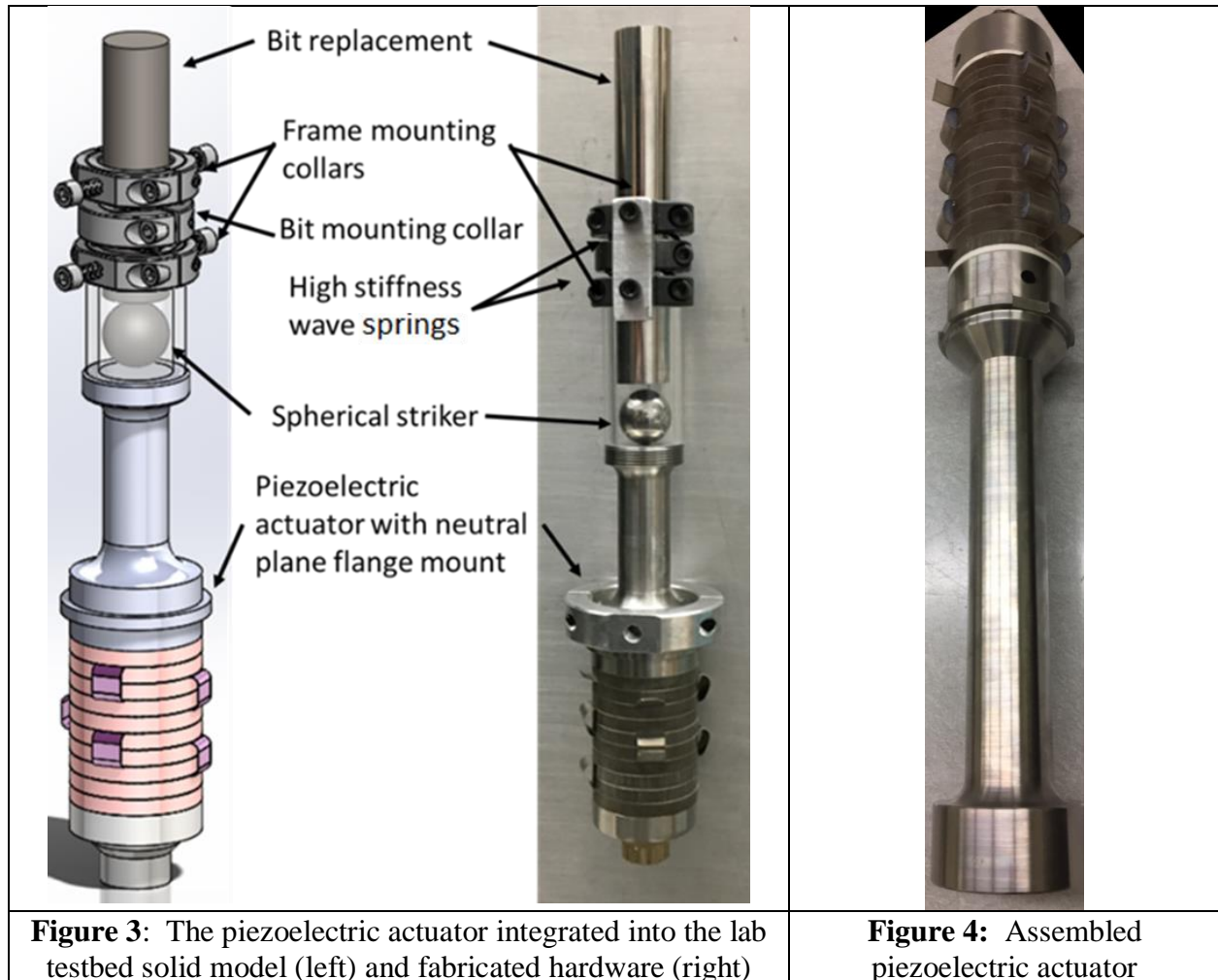


Figure 2: The piezoelectric actuator side view (top) and cross section (bottom)



The 5 kHz actuator and a testbed that was constructed allowed for the testing of the actuator performance with respect to the impact energy (**Figure 5**). The testbed includes a vertically mounted plate on which the actuator is mounted at the neutral plane flange. The testbed was updated to have the actuator mounted with the horn tip facing down to include a preload spring as it is in the drill system implementation. A solid rod is used as a bit replacement and was mounted between two high stiffness wave springs preloaded between two plate-mounted collars. The gap between the bit replacement and the striker could be adjusted to determine an optimal value where the striker reaches resonance. In **Figure 5**, the implementation system is shown integrated into the impact testbed.

Preliminary test results are currently being acquired and the results are quite promising. The striker tested has a ball shape and two sets of materials were tested: 440C stainless steel and tungsten. The impact energy is calculated using the gap size, impacts frequency and the striker mass. In an initial implementation a PCB force sensor was used for measuring the striker impacts. The relatively high impact forces have damaged the PCB force sensor and efforts are currently underway to replace it with a non-contact optical sensor or accelerometer.

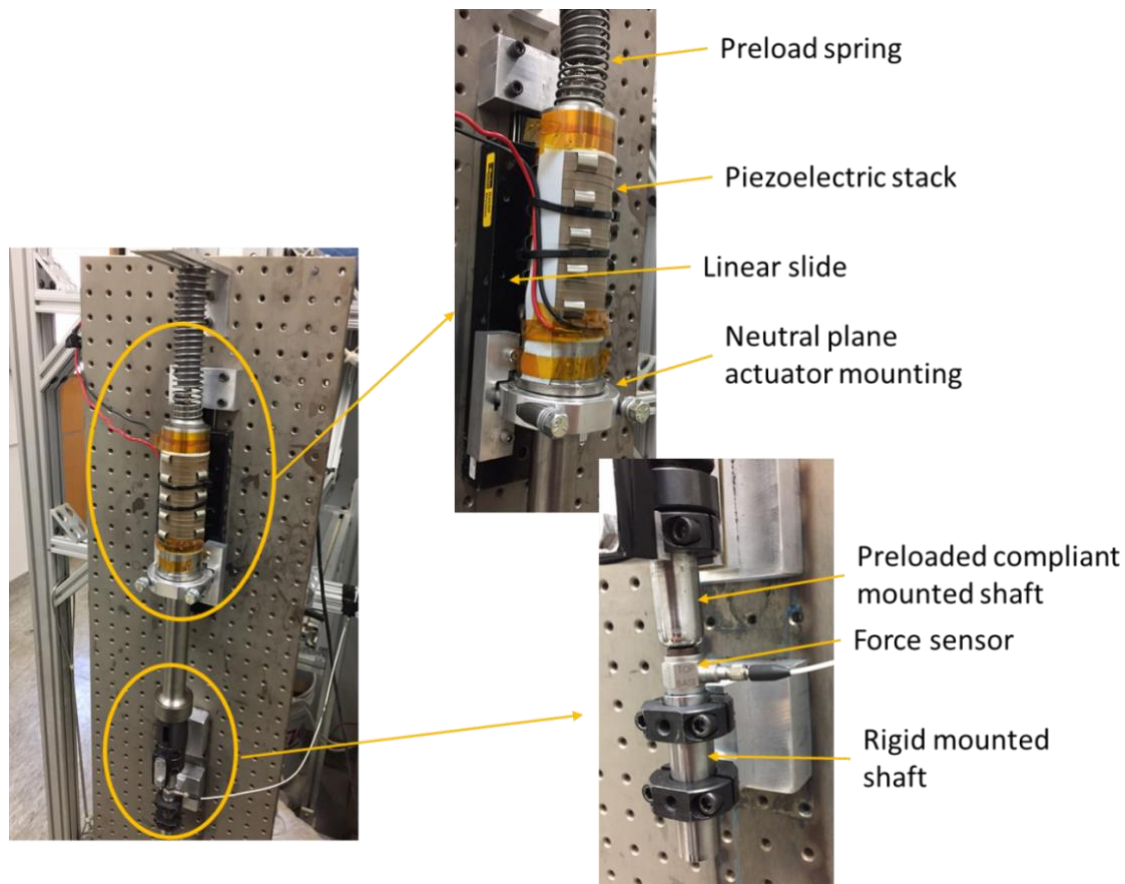


Figure 5: Piezoelectric actuator testbed

ELECTRONICS DRIVER

The goals for the electronic driver is to enable use of the bus drive voltage that is provided from the drill power source. Unlike most high power piezo drivers, the specific driver design that is being developed produces modified square-waves rather than sine waves. This transformer-less design improves efficiency while greatly reduces the electronics size and weight. The driver needs to work at the temperature range of $-100\text{ }^{\circ}\text{C}$ to $100\text{ }^{\circ}\text{C}$ and fit in the space allocated inside the drill body. This effort led to the development of firmware to test the drive of the actuators and to explore packaging possibilities. The focus has been on the ability to operate over large temperatures while delivering 300W of power to a piezo stack with minimal heat dissipation and reliable communications with the drive electronics. The driver performance was tested with great results using a vertically mounted 5 kHz piezoelectric transducer and a bearing ball spherical striker. During the early tests, the free-mass ball was lifted over 6-inches completely out of its retaining tube. However, this test also had uncovered a shortcoming in the drive electronics - the resolution of the 50Hz frequency steps produced by the micro-controller were not sufficiently enough to fine-tune the resonance. Therefore, a programmable oscillator was implemented which now gives the driver frequency steps down to 1Hz.

The new driver version includes temperature sensors with improved noise immunity, better opto-isolators and the addition of a filter choke between the low and high voltage sections. To evaluate these changes, tiny daughter-boards were added on the top of board Version 1, while the filter choke was installed on the bottom (see **Figure 6 top**). Continued testing exposed further weaknesses of overheating and, therefore, another circuit was also built on a daughter-board to

reduce its resistance. The current sense overheat was corrected by using a higher wattage resistor. With the addition of an RS485 transceiver IC, the overall electronic design became ready for the fabrication of the new PCB Version 2. All of the upgrades used during the tests of board Version 1 were incorporated into the new design without having to change the board dimensions. Testing of the new board shows good overall performance while running at high drive power without the need for any changes.



Figure 6: Electronic driver board Version 1 (top) and 2 (bottom)

The communication between the piezo controller and the full system is an RS-485 interface using the MODBUS ASCII communication protocol. In order to ensure a smooth operation the system processor was emulated and software libraries were developed. The software is being developed in three main modules: MODBUS ASCII module, error-logging module, and the Gopher command module. The MODBUS module was written to implement the MODBUS ASCII standard, perform error checking, and simplify the interface between the Gopher module and the piezo microcontroller. The error-logging module assists with time stamping, formatting, and piping events to desired locations, which is very beneficial for trouble shooting. The gopher command module implements the long MODBUS ASCII commands as simple function calls with arguments.

THE BIT CONFIGURATION

The bit is the end-effector that enables the penetration of formation and the removal of the cuttings. Initially, the focus has been on using a coring bit but it was determined that it is a great challenge to assuring the removal of the cores throughout the process of reaching great depths. Therefore, the authors changed the focus to the use of an auger as a means of fragmenting the penetrated formation and uploading it to the surface. However, removal of cuttings in the form of soil poses a challenge in enabling to retain them till the drill is uploaded to the surface. Two drill bit design configurations were proposed and one was decided to be implemented further. A first configuration (**Figure 7**) includes a single row drill bit head, a cylindrical bit barrel and interface to the rotating drill housing and impacts of the striker. This solution was decided to be implemented further for its simplicity. A second solution includes an inner central rod that transfers the impacts from the striker to the drill bit head. The drill bit head is attached to the bit barrel using a flexure

with high torsional stiffness but a low axial stiffness. This configuration allows for lower loss in the impact energy during the transfer to the drill head.

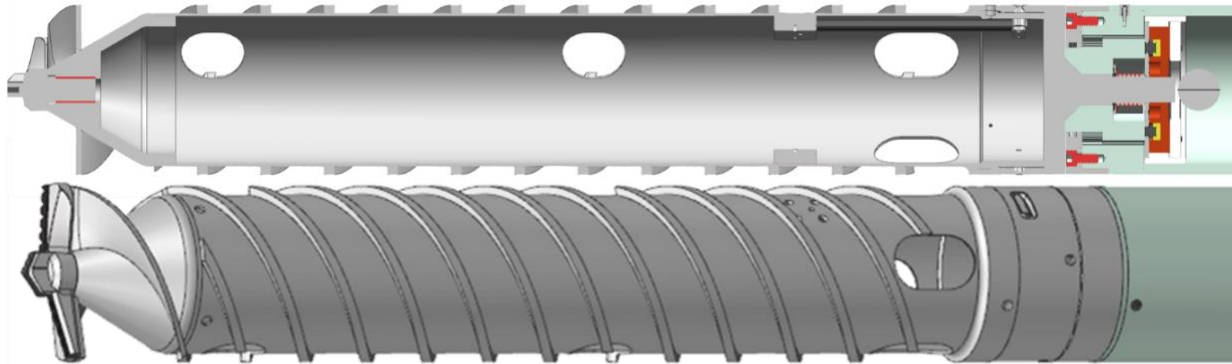


Figure 7: Bit design and interface to the rotating drill housing and striker impacts shown in cross section (top) and isometric view (bottom)

Currently, single row drill bit head, a cylindrical bit barrel and interface to the rotating drill housing and impacts of the striker are implemented. Also, impact analysis is being conducted using parameters that were extracted from the design and they are used. Fabrication of the current design implementation will be based on the test results.

To study the hammering behavior of the bit, a Finite Element (FE) model was established. It is an axisymmetric model that includes a steel ball having 3.8 cm (1.5 inch) diameter, drill bit and a block of rock as shown **Figure 8**. The real teeth of the bit are arranged in a straight line across the diameter of the bit with a thickness of 3 mm. In the model, the teeth are assumed to be arranged in a circle of the same length as the straight line and with the same thickness. This modification makes the teeth shape compatible with the axisymmetric model and maintains the same contact area with the rock.

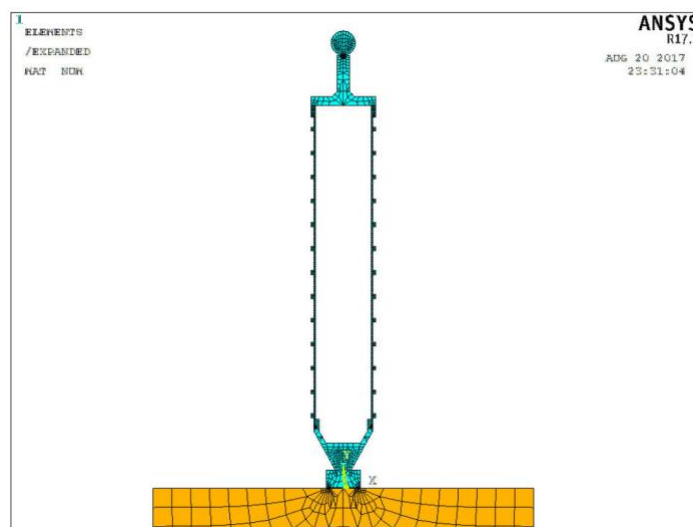


Figure 8: The FE model of the drill bit impacted by a ball

In the simulation, the ball is hitting the shaft of the bit with a speed of 3 m/s. The corresponding energy is 1 J. **Figure 9** shows the displacements of the ball and the bit shaft. The contact time is $\sim 125 \mu\text{s}$ and the bouncing back speed was calculated as 1.83 m/s. The force at the ball-bit and the bit-rock interfaces are presented in **Figure 10**. The maximum ball impact force reaches 16.7 kN at time of $\sim 50 \mu\text{s}$. The impact creates an elastic wave that is propagating down into the rock. The maximum force at the bit-rock interface is up to 22.1 kN (65 MPa averaged stress) at $\sim 280 \mu\text{s}$. The stress itself may fracture rocks having medium hardness.

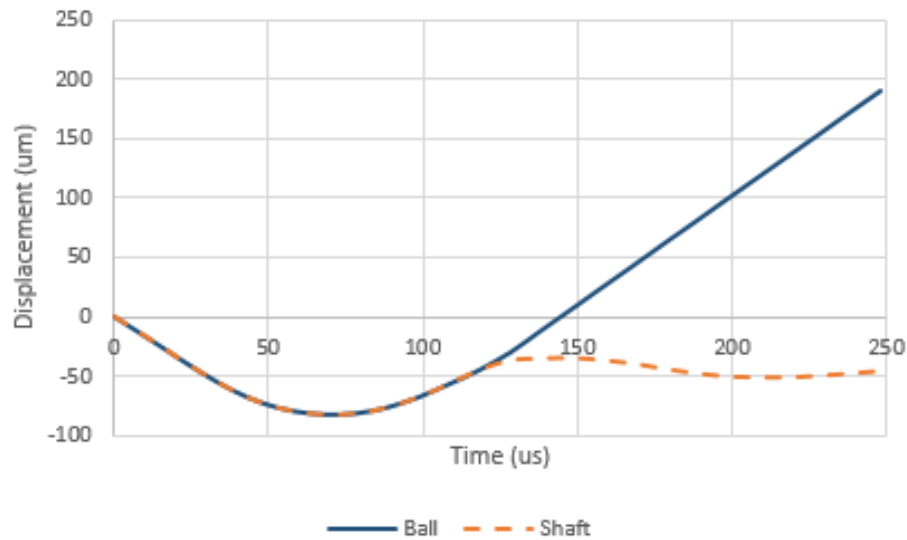


Figure 9: The displacements of the ball and bit shaft after impact.

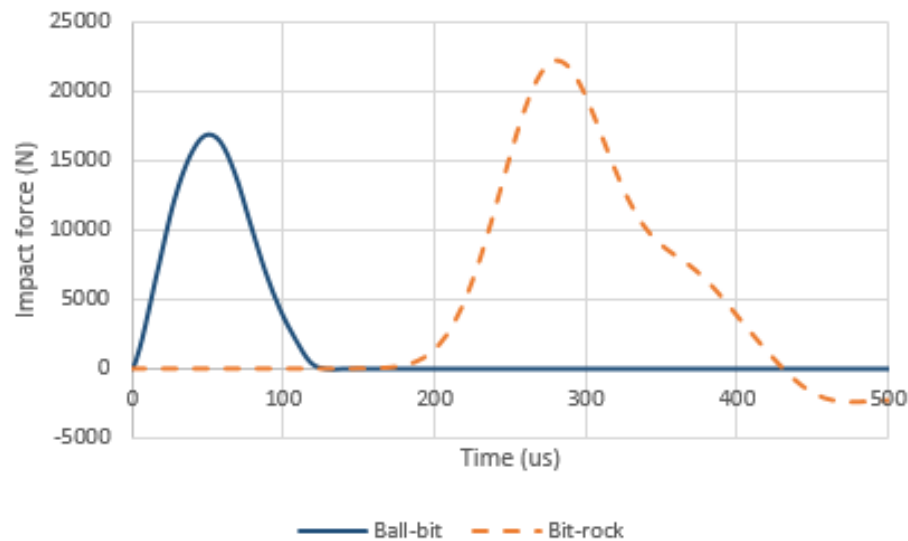


Figure 10: The force at the ball-bit and the bit-rock interfaces

CONCLUSIONS AND FUTURE WORK

In this paper, we presented the current state of development of the piezoelectric transducer for the Auto-Gopher-II, including the drive electronics. Testing of an initial 10 kHz transducer suggested that the momentum transfer to the free mass was not sufficient to produce fracture stress at the rock bit interface. The testing of a modified 5 kHz transducer showed impact energies at the 1 J

level. In parallel, we are working on the development of an effective drill bit configuration, integrating it with the transducer and testing it with the developed drive electronics. After preliminary tests completion the hardware and drive electronics will be integrated and will be tested both in the lab and in the field.

ACKNOWLEDGEMENTS

Research reported in this abstract was conducted at the Jet Propulsion Laboratory (JPL), California Institute of Technology, jointly with Honeybee Robotics under a contract with National Aeronautics Space Administration (NASA). This research is funded by the NASA's MatISSE (Maturation of Instruments for Solar System Exploration) program.

REFERENCES

- Badescu, M., Sherrit, S., Olorunsola, A.K., Aldrich, J., Bao, X., Bar-Cohen, Y., Chang, Z., Doran, P.T., Kenig, F., Fritsen, C., Murray, A., McKay, CP., Peterson, T., Du, S., Tao, S., "Ultrasonic/Sonic Gopher for Subsurface Ice and Brine Sampling: Analysis and Fabrication Challenges, and Testing Results", Proceedings of the SPIE 13th Annual Symposium on Smart Structures and Materials, San Diego, CA, SPIE Vol. 6171-07, 26 February – 2 March, 2006.
- Badescu, M., Kassab, S., Sherrit, S., Aldrich, J., Bao, X., Bar-Cohen, Y., and Chang, Z. (2007). "Ultrasonic/Sonic Driller/Corer as a hammer-rotary drill." Proc., of the 14th International Symposium on: Smart Structures and Materials & Nondestructive Evaluation and Health Monitoring, International Society for Optics and Photonics, 65290S.
- Badescu, M., Sherrit, S., Bao, X., Bar-Cohen, Y., Chen, B., (2011) "Auto-Gopher - a wire-line rotary-hammer ultrasonic drill," Proceedings of the SPIE International Symposium on Smart Structures and Nondestructive Evaluation, SPIE SS11-SSN07-157 7981-135, San Diego, CA, 6-10 March, 2011.
- Bao, X., Bar-Cohen, Y., Chang, Z., Dolgin, B. P., Sherrit, S., Pal, D. S., Du, S., and Peterson, T. (2003). "Modeling and computer simulation of ultrasonic/sonic driller/corer (USDC)." Ultrasonics, Ferroelectrics and Frequency Control, IEEE Transactions on, 50(9), 1147-1160.
- Bar-Cohen, Y., Sherrit, S., Dolgin, B., Bao, X., Chang, Z., Krahe, R., Kroh, J., Pal, D., Du, S., Peterson, T., (2001), "Ultrasonic/Sonic Driller/Corer (USDC) for planetary application," Proc. SPIE Smart Structure and Materials 2001, pp. 529-551.
- Bar-Cohen, Y., and Zacny, K. (2009). Drilling in extreme environments: penetration and sampling on earth and other planets, John Wiley & Sons.
- Sherrit S., X. Bao, Z. Chang, B. Dolgin, Y. Bar-Cohen, D. Pal, J. Kroh, T. Peterson, (2000) "Modeling of the ultrasonic/sonic driller/corer: USDC," 2000 IEEE Int. Ultrason. Symp. Proc., vol.1, pp. 691-694, 2000.